



UvA-DARE (Digital Academic Repository)

Multimodality approach towards individualized non-small cell lung cancer treatment

Schaake, E.E.

Publication date
2014

[Link to publication](#)

Citation for published version (APA):

Schaake, E. E. (2014). *Multimodality approach towards individualized non-small cell lung cancer treatment*. [Thesis, externally prepared, Universiteit van Amsterdam].

General rights

It is not permitted to download or to forward/distribute the text or part of it without the consent of the author(s) and/or copyright holder(s), other than for strictly personal, individual use, unless the work is under an open content license (like Creative Commons).

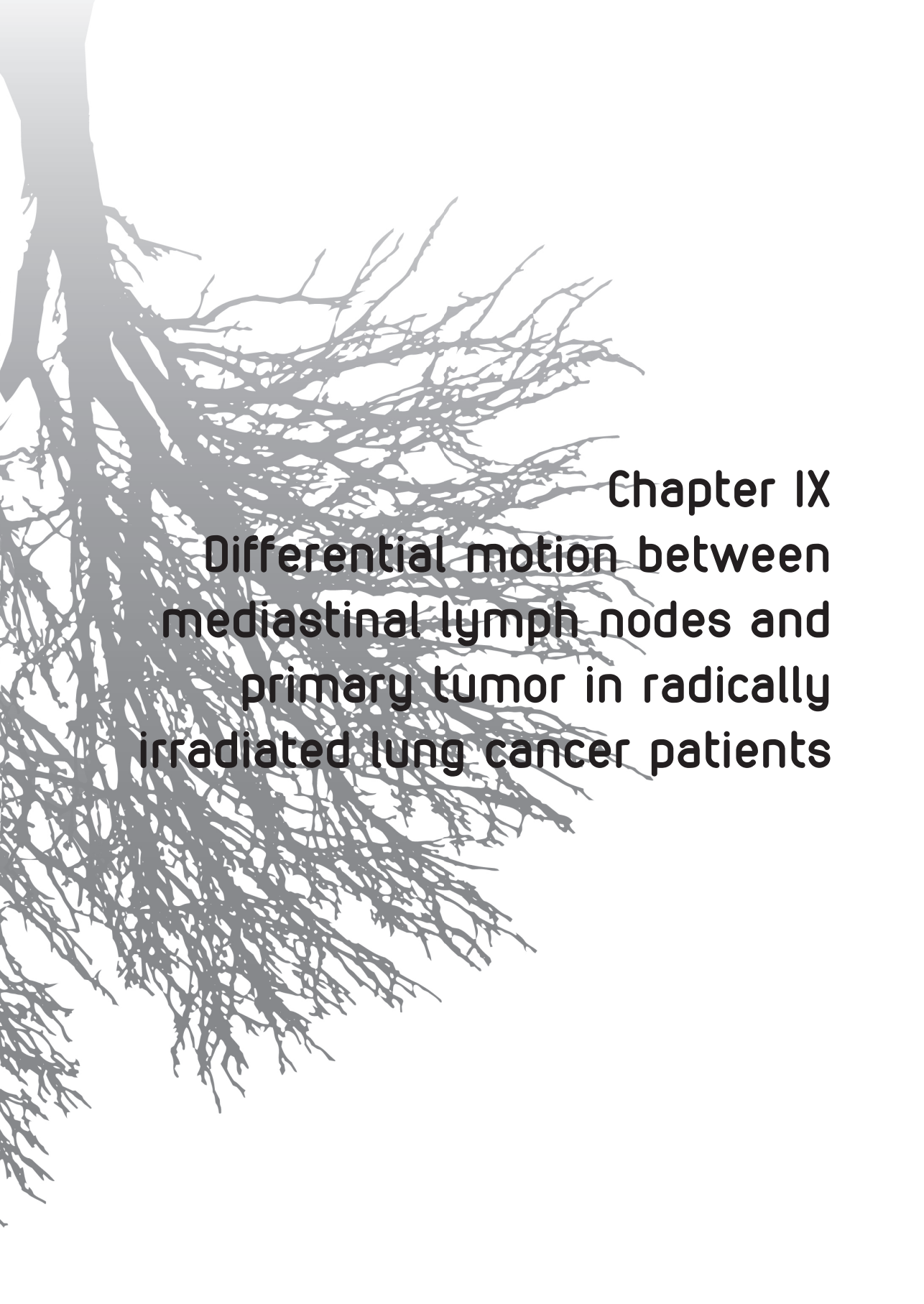
Disclaimer/Complaints regulations

If you believe that digital publication of certain material infringes any of your rights or (privacy) interests, please let the Library know, stating your reasons. In case of a legitimate complaint, the Library will make the material inaccessible and/or remove it from the website. Please Ask the Library: <https://uba.uva.nl/en/contact>, or a letter to: Library of the University of Amsterdam, Secretariat, P.O. Box 19185, 1000 GD Amsterdam, The Netherlands. You will be contacted as soon as possible.



E.E. Schaake
M.M.G. Rossi
W.A. Buikhuisen
J.A. Burgers
A.A.J. Smit
J.S.A. Belderbos
J.-J. Sonke

Submitted



Chapter IX
**Differential motion between
mediastinal lymph nodes and
primary tumor in radically
irradiated lung cancer patients**

ABSTRACT

Purpose/Objective | In locally advanced lung cancer patients, PTV-margins for mediastinal lymph nodes and tumor after a bony anatomy registration based correction protocol typically range from 1-1.5 cm. Detailed information of lymph node motion variability and differential motion in relation to the primary tumor, however, is lacking. In this study lymph node and tumor position variability were analyzed in detail and correlated to the main carina to evaluate if margins can be reduced.

Materials and Methods | Small gold fiducial markers (0.35 x 5 mm) were placed in a mediastinal lymph node of 51 non-small cell lung cancer patients, during a routine diagnostic esophageal or bronchial endoscopic ultrasound (EUS/EUBS) procedure. A 4D-planning (p)CT and daily 4D-CBCT scans were acquired prior to and during radical radiotherapy (66Gy/24fractions). Each CBCT was registered in 3D (bony anatomy) and 4D (tumor, marker and carina) to the pCT. Subsequently, systematic and random residual misalignments of the time-averaged lymph node and tumor position relative to the bony anatomy and carina were determined. Additionally, tumor and lymph node respiratory amplitude variability was quantified. Finally, required margins were quantified using a recipe for dual targets.

Results | Relative to the bony anatomy, the grand mean lymph node displacement was <0.05 cm in all directions, while systematic- and random errors ranged from 0.16-0.32 cm for the markers and 0.15-0.33 cm for the tumor. A large systematic variability in lymph node amplitude between patients was observed with an average motion of 0.56 cm in Cranial-Caudal (CC) direction. Margins could be reduced by 10% Left-Right (LR), 27% CC and 10% Anterior-Posterior (AP) for the lymph nodes and -2%, 15% and 7% for the tumor if an online carina registration protocol replaced a bone registration based protocol.

Conclusions | Detailed analysis revealed considerable lymph node position variability, differential motion and respiratory motion. PTV-margins can be reduced up to 27% in lung cancer patients when the carina registration replaces bony anatomy registration.

INTRODUCTION

Mediastinal lymph node metastasis invasion strongly correlates with the life expectancy in lung cancer patients (1). When mediastinal lymph nodes are involved the treatment of choice consists of concurrent chemoradiation of the primary lung tumor and affected mediastinal lymph nodes. For optimal irradiation, it is necessary to adequately account for geometrical uncertainties such as baseline shifts, differential and respiratory motion (2). Traditionally, generous safety margins are applied to account for such geometrical uncertainties in the absence of adequate correction strategies exposing nearby organs at risk to high radiation doses resulting in considerable toxicity (3-7) such as esophagitis and pneumonitis. Lymph nodes are soft tissues surrounded by vessels and other 'soft' mediastinal tissues, and therefore difficult to localize on in-room imaging series such as Cone Beam CT scans. It is therefore unclear if current Planning Target Volume (PTV) margins of involved lymph nodes sufficiently account for their variability. Current margins are based on tumor position variability only.

In a previous proof of principle analysis of a first patient group of 14 patients, we showed that it is feasible and easy to place gold fiducial markers in mediastinal lymph nodes during routine diagnostic endoscopic ultra sound procedures (8). Subsequently, the cohort was extended to 51 patients to improve statistical power, quantify differential motion between lymph nodes and primary tumor, evaluate intra-fraction variation and registration accuracy, and finally properly advise on margins. The lymph nodes were mapped according to Naruke with different stations (9). The International Association for the Study of Lung Cancer (IASLC) adopted this into a lymph node map (10).

The aim of this study was to perform a detailed analysis of lymph node and primary tumor position variability, differential motion and required safety margins.

MATERIALS AND METHODS

A single center prospective cohort study, opened in 2010, was performed in Non-Small Cell Lung Cancer (NSCLC) patients planned for radical radiotherapy to determine mediastinal lymph node position variability using gold fiducial markers (0.35 mm x 5.0 mm, RadioMed, Barlett, USA; from now on referred to as "marker"). Patients who were medically fit (WHO 0-2), 18 years or older, without prior mediastinal surgery or chest irradiation and who underwent endobronchial ultrasound (EBUS)- or trans-esophageal endoscopic ultrasound-guided mediastinal lymph node fine needle aspiration (EUS-FNA) (11) for diagnostic purposes and were scheduled for radical radiation therapy or chemoradiation as primary treatment, were eligible for inclusion in this study. Written informed consent was obtained from all patients according to the International Conference of Harmonization/ Good Clinical Practice (ICH/GCP) and national and local regulations. This study was approved by the institute's medical ethical committee.

The primary endpoint of the study was to quantify lymph node position and motion variability over the course of radiotherapy in NSCLC patients.

Radiotherapy preparation

Every patient received radical Intensity Modulated RT to a dose of 66 Gy in 24 fractions with an overall treatment time of 32 days. Patients were stabilized by an armrest (In house modified armrest of Civco, Orange City, Iowa, USA) and knee support (Civco). The treatment schedule could be adjusted based on inclusion in clinical trials, mean lung dose or on the patient's comorbidity. A 4D planning CT-scan with intravenous contrast (0.3 cm slice thickness) was acquired and the Mid-Position (MidP)CT scan was subsequently reconstructed (12) for delineation and dose calculation. The planned dose distribution encompassed the primary tumor and pathological or suspect, FDG-PET positive, lymph nodes. The CTV-to-PTV margin was 12 mm for the lymph nodes, while for the primary tumor the CTV-to-PTV margin was $12 \text{ mm} + 0.25A$, with A being the GTV's peak-to-peak amplitude derived from the 4D planning CT. Daily 4D-CBCT scans were acquired and bony anatomy registration was used for online set-up error correction. Once a week, a CBCT scan was performed immediately after treatment delivery to quantify the intra-fraction motion.

Lymph node and tumor position variability analysis

Lymph node marker registration was described previously (8). In short, for each phase of a 4D-CBCT scan the position of the marker was local-rigidly registered (translations only) to the planning CT and the time-weighted mean lymph node position was calculated corrected for bony anatomy misalignments. Additionally, the peak-to-peak breathing amplitude was calculated by its excursion over the phases. Inter-fractional variability was quantified in terms of grand mean (GM), systematic errors (Σ), and random errors (σ). The combined effect of intra-fractional variability and registration inaccuracy was assessed by the difference between pre- and post-treatment CBCT scan registrations corrected for the prescribed couch shift.

In a similar way, the main carina and tumor displacements were quantified by a local rigid 4D grey-value registration. Analysis of the registration accuracy using a 4D adapted full-circle method is described in the Appendix. Additionally, a carina based correction protocol was simulated and residual marker and tumor position variabilities were quantified and compared with the bony anatomy based protocol. The correlation between the marker and the tumor motion variability was analyzed for both a bony anatomy and carina based online correction strategy. Analysis was performed in Matlab 7 (The MathWorks Inc., Natick, MA, 2000). Differences in grand mean, systematic and random variations were tested using the student t-test, chi-square test and sign rank test respectively.

Margins

Traditionally, PTV margins are calculated for a single target. In this paper, two separate targets are analyzed. The derived PTV margin M to ensure that the lymph nodes and the primary tumor simultaneously receive at least 95% of the prescribed dose for 90% of patients was calculated as: $M=2.79 \cdot \Sigma + 1.64 \cdot (\sqrt{[\sigma^2 + \sigma_p^2]} - \sigma_p)$.

The factor 2.79 instead of the more familiar 2.5 was taken from table 2 in the paper of van Herk et al. for a 3D error distribution and a confidence level of $\sqrt{0.9} \approx 0.95$ conservatively assuming uncorrelated uncertainties between lymph nodes and primary tumor (13). The overall systematic and random errors were calculated as $\Sigma = \sqrt{[\Sigma_B^2 + \Sigma_{TD}^2 + \Sigma_L^2 + \Sigma_I^2]}$ and $\sigma = \sqrt{[\sigma_B^2 + \sigma_L^2 + \sigma_I^2 + \sigma_R^2]}$, where the subscript B refers to baseline variation, TD refers to target definition uncertainty (14), L refers to localization accuracy, I refers to intra-fractional variability and R refers to respiratory motion. In this study, σ_R will be approximated by $A/3$, with A the peak-to-peak amplitude. For the lymph nodes $\sigma_p = 0.32$ cm (15) and for the primary tumor $\sigma_p = 0.64$ cm were used to describe the width of the penumbra (16).

RESULTS

Between September 2010 and August 2013 markers were placed in 63 patients. Fifty-four of these patients actually received radical irradiation. Three of these patients could not be analyzed due to inconsistency in the protocol logistics and were excluded. The EUS and EBUS guided marker placement occurred without complications and no markers were lost during placement or treatment.

Patient and tumor characteristics of the 51 patients analyzed are listed in Table 1. All inserted markers were well visible on planning CT and CBCT (Fig 1). An average of 22 CBCT scans was acquired per patient (range 17-24). Intra-fraction motion was measured in 49 patients with an average of 4 post treatment CBCT's per patient (range 3-6).

Lymph node and primary tumor variation

Grand mean baseline variation was statistically insignificant and ≤ 0.05 cm in all directions for both lymph nodes and tumor (Table 2A). The systematic baseline variation ranged from 0.20-0.32 cm for the markers and 0.15-0.33 cm for the tumor. Random errors were up to 25% smaller than systematic errors.

The mean peak-to-peak amplitude of the lymph nodes during treatment was 0.56 cm in the CC direction and on the population level very similar to that of the tumor: 0.55 cm (Table 3). Grand mean differences relative to the 4D planning CT scan were negligible for the Left-Right (LR) and Antero-Posterior (AP) direction while statistically significant for the CC direction: -0.08 cm (13% smaller during treatment; $p=0.04$) for the markers and -0.13 cm (24% smaller during treatment; $p=0.002$) for the tumor. The systematic amplitude differences ranged from 0.19-0.27 cm for the markers and 0.12-0.28 cm for the tumor. Random variations were typically 40-53% smaller. Registration accuracy was analyzed and was below 1 mm SD for all structures (Appendix). It therefore has a

Table 1: Characteristics of the patients analyzed.

Patient characteristics	All patients (n = 51)	
	N= or Median	% or range
Age	64	36-85
Gender		
Male	27	53
Female	24	47
Stage		
IA	0	0
IB	1	2
IIA	3	6
IIB	2	3
IIIA	24	46
IIIB	20	38
IV	1	2
Histology/Cytology		
Adeno carcinoma	15	30
Squamous cell carcinoma	19	37
Undifferentiated NSCLC	17	33
Radiation dose		
Number of fractions	24	17-30
Fraction dose	2.75	2-3.4
Marker in lymph node stations (n=)		
II Left	6	12
IV Left	11	22
IV Right	10	20
V	2	4
VII	17	33
VIII	2	4
XI	3	6
Chemotherapy		
None	5	10
Concurrent daily low dose cisplatin	44	86
other	2	4

*Table 2A+B: Inter-fraction position variability relative to bony anatomy and carina.**Table 2A: Grand mean, systematic and random baseline variability of the lymph nodes and tumor after bony anatomy based corrections.*

		LR (cm)	CC (cm)	AP (cm)
Marker:	GM	-0.023	0.040	-0.048
	Σ	0.20	0.32	0.21
	σ	0.19	0.24	0.16
Tumor:	GM	0.004	0.049	-0.031
	Σ	0.15	0.33	0.23
	σ	0.16	0.26	0.25

Table 2B: Grand mean, systematic and random baseline variability of the bony anatomy, lymph nodes and tumor after carina based corrections.

		LR (cm)	CC (cm)	AP (cm)
Bone:	GM	0.041	-0.033	0.001
	Σ	0.12	0.28	0.17
	σ	0.15	0.21	0.14
Marker:	GM	-0.018	0.007	-0.048
	Σ	0.15	0.13	0.16
	σ	0.13	0.14	0.12
Tumor:	GM	0.036	-0.016	-0.031
	Σ	0.16	0.24	0.20
	σ	0.18	0.21	0.21

limited impact on these results.

Carina based corrections

Carina based corrections successfully reduced the inter-fractional position variability of both lymph nodes and tumors compared to a bony anatomy based correction (Table 2b). For the markers these reduction were 22% (LR;p=0.09), 59% (CC;p<1e-4) and 24% (AP;p=0.06) systematically and 33% (p<1e4) 40% (p<1e4) 24% (p=0.002) randomly. For the tumor this was -3.9% (p=0.79), 27% (p=0.03) and 13% (p=0.35) systematically and -9.7% (p=0.88), 19% (p=0.0002) and 16% (p=0.005) randomly. Note that a carina based correction protocol induces variability of the bony anatomy that otherwise would be near-perfectly positioned with systematic and random variability ranging from 0.12-0.28 cm.

Table 3: Inter-fraction peak-to-peak amplitude statistics for the population and grand mean (GM), systematic (Σ) and random (σ) amplitude changes relative to the 4D planning CT for both the marker and the primary tumor.

Amplitude statistics		LR (cm)	CC (cm)	AP (cm)
Marker:	Population Mean	0.23	0.56	0.24
	Population Min	0.10	0.12	0.10
	Population Max	0.50	1.7	0.53
	GM	0.002	-0.08	-0.01
	Σ	0.19	0.27	0.19
	σ	0.1	0.13	0.11
Tumor:	Population mean	0.14	0.55	0.21
	Population Min	0.03	0.04	0.06
	Population Max	0.35	2.26	0.74
	GM	-0.02	-0.13	-0.02
	Σ	0.12	0.28	0.14
	σ	0.07	0.13	0.08

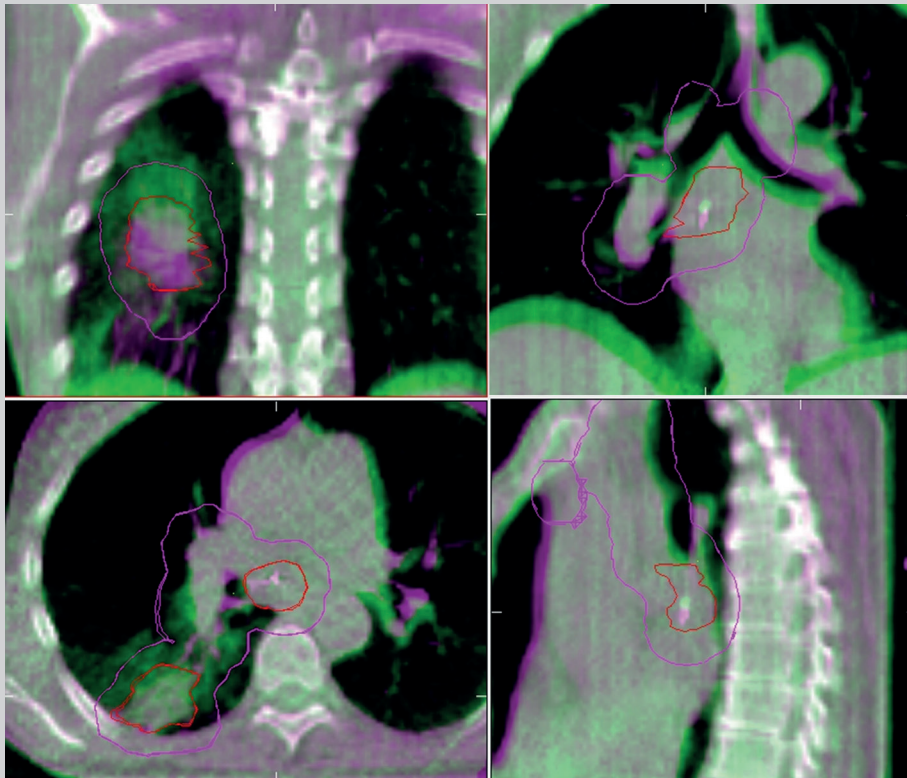


Figure 1: Color fusion of a MidP planning CT (purple) and single phase of a 4D CBCT (green) illustrating a baseline shift of both lymph node (green purple marker displacement visible in coronal and sagittal view, top and bottom right) and primary tumor (large green purple tumor displacement visible in coronal view, top left).

Table 4A+B: Intra-fraction position and amplitude variability

	LR (cm)	CC (cm)	AP (cm)
Marker: GM	0.012	0.085	-0.057
Σ	0.19	0.17	0.15
σ	0.17	0.21	0.15
Tumor: GM	0.019	0.067	-0.07
Σ	0.18	0.19	0.16
σ	0.16	0.21	0.16

Table 4A: Grand mean, systematic and random intra-fraction position variability.

	LR (cm)	CC (cm)	AP (cm)
Marker: GM	0.005	-0.043	0.012
Σ	0.07	0.10	0.08
σ	0.13	0.17	0.14
Tumor: GM	-0.017	-0.046	-0.012
Σ	0.03	0.09	0.04
σ	0.05	0.13	0.07

*Table 4b: Grand mean, systematic and random intra-fraction amplitude variability:**Intra-fraction variation*

Intra-fraction variability was considerably smaller than inter-fraction variability (Table 4A+B). Nevertheless, the sub-millimeter grand mean values were statistically significant for the CC and AP direction for both the markers and the tumor indicating a small drift to the cranial and posterior side. Systematic and random intra-fraction variations ranged from 0.15-0.21cm and were 20-45% smaller than inter-fractionally.

Intra-fraction amplitude variation was also quite small with grand mean changes <0.05cm and systematic variation <0.1 cm. Random amplitude variations were somewhat larger up to 0.17 cm but likely affected by the registration accuracy of 0.15 cm as described in the Appendix.

Correlation marker-tumor

The correlation between the marker and tumor systematic position variability was determined in the 3 orthogonal directions. For the bony anatomy based correction protocol, these correlations were: 0.17 (LR;p=0.23), 0.71 (CC;p<1e-4) and 0.55 (AP;p=<1e-4). For a carina based correction protocol the correlations were: -0.06 (LR;p=0.69), 0.21 (CC;p=0.16) and 0.34 (AP;p=0.016).

Margins

The required PTV margins depend on the delineation accuracy, patient's respiratory motion and correction strategy. In Figure 2, the required PTV margins are shown for both the lymph nodes and tumor for varying amplitude and delineation uncertainties. For the population average respiratory amplitudes and an assumed target definition uncertainty $\Sigma TD=0.2\text{cm}$ (17) (valid for parts of the tumor with a very clear boundary) the bone-based margins are 1.1cm(LR), 1.4cm(CC) and 1.0cm(AP) for lymph nodes and 0.9 cm(LR), 1.4cm(CC) and 1.1cm(AP) for tumor. For a carina registration based correction strategy margin reduction of 10%, 27% and 10% for the lymph nodes and -2%, 15% and 7% for the tumor are achievable.

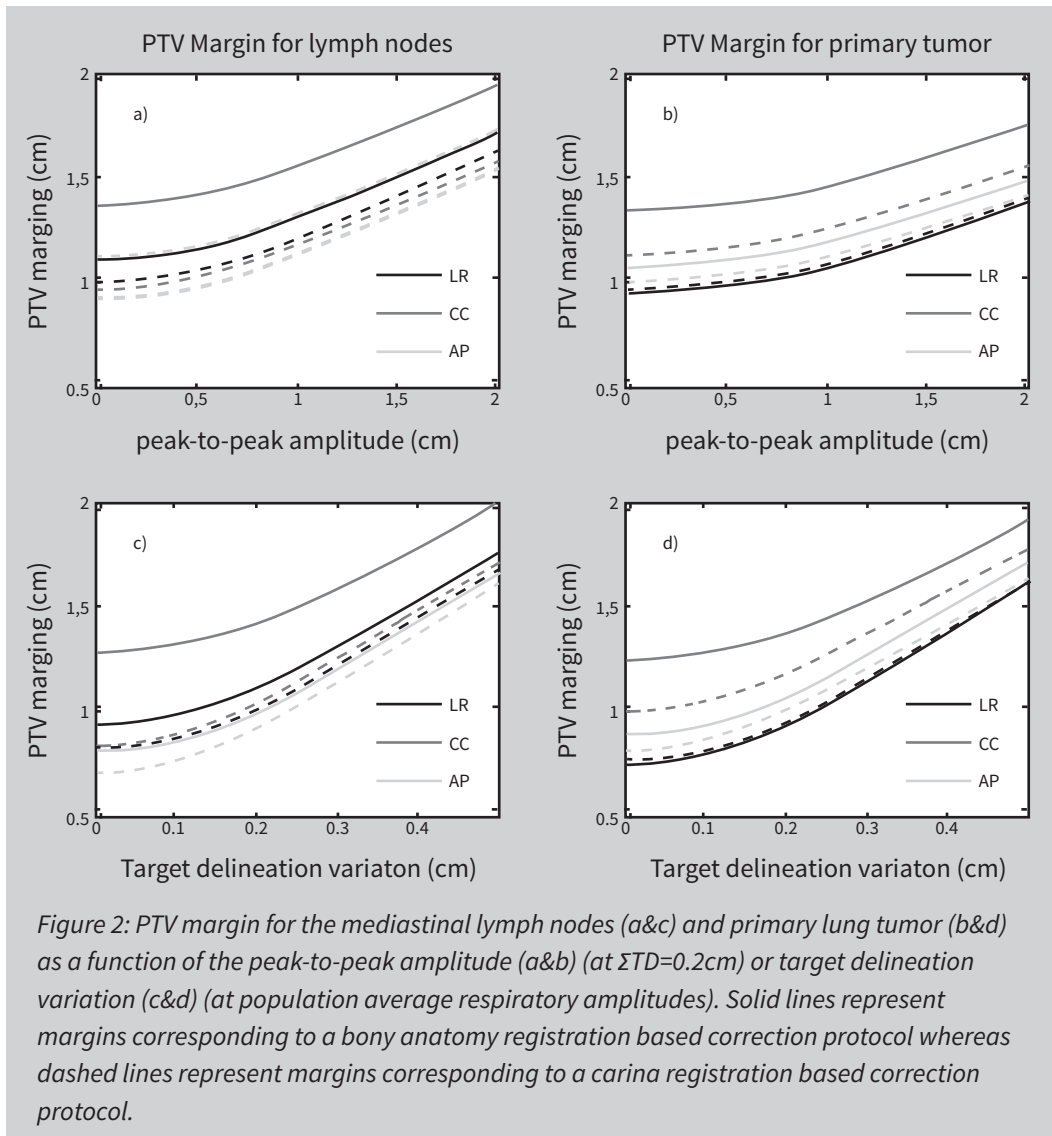


Figure 2: PTV margin for the mediastinal lymph nodes (a&c) and primary lung tumor (b&d) as a function of the peak-to-peak amplitude (a&b) (at $\Sigma TD=0.2\text{cm}$) or target delineation variation (c&d) (at population average respiratory amplitudes). Solid lines represent margins corresponding to a bony anatomy registration based correction protocol whereas dashed lines represent margins corresponding to a carina registration based correction protocol.

DISCUSSION

Lymph node and tumor position variability and differential motion were analyzed in detail. Using a margin recipe for multiple targets, a carina registration based correction strategy was shown to be superior to a bony anatomy registration strategy. Margins can be decreased up to 32% in the CC direction by using the main carina instead of the bony anatomy as a surrogate for the tumor and lymph nodes.

In the recent years a few studies have been published that quantify lymph node position variability. The inter-fraction variability of lymph nodes found in this study was up to 1 mm different compared to our proof of principle paper with only 14 analyzed patients (8). This could be expected with the low number of included patients in the pilot study. Similarly, Jan et al. (18), Roman et al. (19) and Weiss et al. (20) published analyses on small patient cohorts based on delineated structures and/or weekly scans reporting similar (19) or larger variability than found in this study (18, 20), likely due to delineation uncertainty and/or limited statistical power. In patients without large anatomical changes, however, Weiss et al. found somewhat smaller variability.

The systematic amplitude variability was larger than the random variability illustrating the imperfection of the 4DCT based amplitude assessment during treatment preparation which is based on a single respiratory cycle and thus more susceptible to breathing irregularities compared to 4D-CBCT scans which are based on dozens of cycles. As well there was a small reduction of the average amplitude. The 4D-CT was obtained using a respiratory sensor (a thermocouple inserted into the entry of a regular oxygen mask) which possibly influences the respiratory behavior while being absent during 4D-CBCT acquisition. The low random amplitude variability of both tumor and lymph nodes amplitude illustrates the day-to-day stability of the patient's respiratory behavior which is in line with observations by Sonke et al. (16) and Rit et al (21).

In this study, intra-fraction variability was measured weekly using a pre-treatment and post-treatment scan. The variability assessed by this post-treatment scan therefore is the combined effect of imperfect corrections (localization variability) and position changes during treatment delivery (true intra-fraction motion). This might explain that the reported intra-fractional position variability is somewhat larger than intra-fractional variability reported for SBRT (22), despite the shorter delivery time for conventionally fractionated RT.

The intra-fraction amplitude variability was generally quite small, but the random intra-fraction amplitude variability of the lymph nodes was larger than the inter-fraction variability. Note, however, that the intra-fractional variation is the result of the difference in amplitude in the pre-correction and post treatment scan and thus more susceptible to measurement uncertainties as described in the Appendix.

The carina registration based correction strategy allows considerable margin reduction compared to a bony anatomy based registration method and was most

effective in the CC direction, both for the lymph nodes and the primary tumor. The required margin we calculated (Fig 2) increased more rapidly with respiratory amplitude for the lymph nodes than for the tumor. This is due to the sharper penumbra (σ) modeled for the lymph nodes. It is assumed here that the lymph nodes are surrounded by water equivalent material while the tumor is surrounded by lung. If the tumor is adjacent to the mediastinum or thorax wall, somewhat larger margins are required.

Some limitations of this study are: gold markers were used as a surrogate of the lymph node position, yet markers are no lymph nodes. However, a marker is potentially more representative than a delineation of the very low contrast structure, although anatomical changes within the lymph node and registration errors may occur while matching the markers. To optimize margins and reduce uncertainties, an online correction protocol is in use since January 2012 for patients with lung cancer slightly increasing the workload for a lung cancer irradiation course.

Only a limited amount of lymph node stations were reached by EUS and EBUS. We have therefore not been able to distinguish the differences in position variability for different lymph node stations.

Not all patients receiving a marker were suitable for analysis or received radical irradiation. In one patient, EUS revealed disease negative lymph nodes and a radical resection was the preferred treatment; the marker was removed during the lymph node dissection with surgery. Seven other patients did not receive radical irradiation due to metastatic disease discovered during work-up and therefore could not be analyzed.

Daily online CBCT became standard practice following our pilot study that indicated that our lymph node margins were inadequate for offline correction protocol. Besides more accurate positioning, such an online protocol allows close monitoring of anatomical changes such as increased/decreased atelectasis and pleural effusion and associated displacements of the treatment targets, either tumor or lymph nodes. Such changes over the course of treatment can be resolved with adaptive radiotherapy. Based on this study, a carina registration based correction protocol has been clinically implemented, replacing the previous bony anatomy based protocol in our institute. So far, however, PTV margins have not yet been changed. Note that a carina registration based correction protocol increases the position variability of the spinal cord compared to an online protocol based on bony anatomy. On the other hand, the resulting position variability is quite similar to those reported for an offline bony anatomy based protocol and thus similar planning tolerance limits may be applied.

We have shown that a carina based correction protocol allows reducing margins and thereby reducing toxicity in the mediastinum, without expecting a decrease in local control. This hypothesis should, however, be tested in a clinical trial as it may affect control of microscopic disease.

REFERENCES

1. Dehing-Oberije C, De RD, van der Weide H, et al.: Tumor volume combined with number of positive lymph node stations is a more important prognostic factor than TNM stage for survival of non-small-cell lung cancer patients treated with (chemo)radiotherapy. *Int J Radiat Oncol Biol Phys* 70:1039-1044, 2008
2. Sonke JJ, Lebesque J, van Herk M: Variability of four-dimensional computed tomography patient models. *Int J Radiat Oncol Biol Phys* 70:590-598, 2008
3. Graham MV, Purdy JA, Emami B, et al.: Clinical dose-volume histogram analysis for pneumonitis after 3D treatment for non-small cell lung cancer (NSCLC). *Int J Radiat Oncol Biol Phys* 45:323-329, 1999
4. Jenkins P, D'Amico K, Benstead K, et al.: Radiation pneumonitis following treatment of non-small-cell lung cancer with continuous hyperfractionated accelerated radiotherapy (CHART). *Int J Radiat Oncol Biol Phys* 56:360-366, 2003
5. Rancati T, Ceresoli GL, Gagliardi G, et al.: Factors predicting radiation pneumonitis in lung cancer patients: a retrospective study. *Radiother Oncol* 67:275-283, 2003
6. Seppenwoolde Y, Lebesque JV, de Jaeger K, et al.: Comparing different NTCP models that predict the incidence of radiation pneumonitis. Normal tissue complication probability. *Int J Radiat Oncol Biol Phys* 55:724-735, 2003
7. Tsujino K, Hirota S, Endo M, et al.: Predictive value of dose-volume histogram parameters for predicting radiation pneumonitis after concurrent chemoradiation for lung cancer. *Int J Radiat Oncol Biol Phys* 55:110-115, 2003
8. Schaake EE, Belderbos JS, Buikhuisen WA, et al.: Mediastinal lymph node position variability in non-small cell lung cancer patients treated with radical irradiation. *Radiother Oncol* 105:150-154, 2012
9. Naruke T, Suemasu K, Ishikawa S: Lymph node mapping and curability at various levels of metastasis in resected lung cancer. *J Thorac Cardiovasc Surg* 76:832-839, 1978
10. Radiologyassistant.nl: Lymph node station map, in , 2014
11. Lennon AM, Penman ID: Endoscopic ultrasound in cancer staging. *Br Med Bull* 84:81-98, 2007
12. Wolthaus JW, Schneider C, Sonke JJ, et al.: Mid-ventilation CT scan construction from four-dimensional respiration-correlated CT scans for radiotherapy planning of lung cancer patients. *Int J Radiat Oncol Biol Phys* 65:1560-1571, 2006
13. van Herk M, Remeijer P, Rasch C, et al.: The probability of correct target dosage: dose-population histograms for deriving treatment margins in radiotherapy. *Int J Radiat Oncol Biol Phys* 47:1121-1135, 2000
14. McKinzie A: Defining the pTV and prv - new ideas about old problems . *Radiother Oncol* 2004;73(Supplement-1):S203, 2004 (abstr)
15. Witte MG, van der Geer J, Schneider C, et al.: The effects of target size and tissue density on the minimum margin required for random errors. *Med Phys* 31:3068-3079, 2004

16. Sonke JJ, Rossi M, Wolthaus J, et al.: Frameless stereotactic body radiotherapy for lung cancer using four-dimensional cone beam CT guidance. *Int J Radiat Oncol Biol Phys* 74:567-574, 2009
17. Steenbakkers RJ, Duppen JC, Fitton I, et al.: Reduction of observer variation using matched CT-PET for lung cancer delineation: a three-dimensional analysis. *Int J Radiat Oncol Biol Phys* 64:435-448, 2006
18. Jan N, Balik S, Hugo GD, et al.: Interfraction Displacement of Primary Tumor and Involved Lymph Nodes Relative to Anatomic Landmarks in Image Guided Radiation Therapy of Locally Advanced Lung Cancer. *Int J Radiat Oncol Biol Phys*, 2013
19. Roman NO, Shepherd W, Mukhopadhyay N, et al.: Interfractional positional variability of fiducial markers and primary tumors in locally advanced non-small-cell lung cancer during audiovisual biofeedback radiotherapy. *Int J Radiat Oncol Biol Phys* 83:1566-1572, 2012
20. Weiss E, Robertson SP, Mukhopadhyay N, et al.: Tumor, lymph node, and lymph node-to-tumor displacements over a radiotherapy series: analysis of interfraction and intrafraction variations using active breathing control (ABC) in lung cancer. *Int J Radiat Oncol Biol Phys* 82:e639-e645, 2012
21. Rit S, van HM, Zijp L, et al.: Quantification of the variability of diaphragm motion and implications for treatment margin construction. *Int J Radiat Oncol Biol Phys* 82:e399-e407, 2012
22. Guckenberger M, Meyer J, Wilbert J, et al.: Intra-fractional uncertainties in cone-beam CT based image-guided radiotherapy (IGRT) of pulmonary tumors. *Radiother Oncol* 83:57-64, 2007

APPENDIX: REGISTRATION ACCURACY

Registration accuracy was estimated by a ‘full circle method’ (A1). Originally, the full circle method is based on the registration of three scans in a cyclic fashion, where scan 1 is registered to scan 2, scan 2 is registered to scan 3 and scan 3 is registered to scan 1 (Figure A1a). The combined registration result along the circle $C=R_{1\rightarrow 2}R_{2\rightarrow 3}R_{3\rightarrow 1}$ ideally would be zero but in practice a residual remains that characterizes random registration inaccuracies. By performing the circle registration for multiple patients and calculating the standard deviation across the patients yields:

$$SD(C) = SD(3R) = \sqrt{3}SD(R).$$

In this paper, dealing with 4D CBCT data, the full circle method was adapted as depicted in Figure A2b. First, two 4D-CBCT scans were registered phase-by-phase to the 3D MidP planning CT. The time averaged registration result effectively describes the registration of the MidP of the CBCT to the MidP planning CT. Additionally, all phases of CBCT 1 and CBCT 2 were registered to phase 2 of CBCT 2. Subsequently, the circle is described as:

$$C = \left(\sum_{p=0}^9 w_{CBCT1}^p R_{CBCT_1^p \rightarrow pCT} \right)^{-1} \sum_{p=0}^9 w_{CBCT1}^p R_{CBCT_1^p \rightarrow CBCT_2^2} \left(\sum_{p=0}^9 w_{CBCT2}^p R_{CBCT_2^p \rightarrow CBCT_2^2} \right)^{-1} \sum_{p=0}^9 w_{CBCT2}^p R_{CBCT_2^p \rightarrow pCT} ,$$

in which w describes the relative time spent in each phase p . The registrations utilized for the full circle method also include two independent amplitude measurements for both CBCT 1 and CBCT 2. Subtracting these two amplitudes also allows quantification of the accuracy of the amplitude assessment.

The full circle method was applied to 10 patients for each of the Region of Interest (ROI) used in this paper: 3D Rectangular shaped ROI’s were used around the vertebrae (classical 3D full circle method), and the inserted marker and carina (4D Registration). Finally, a shaped ROI around the GTV was used with 4D registration. Both the registration variability (1 SD) for the time averaged mean position and the amplitude are shown in Table A1. The average over the evaluated patients was sub-millimeter in all directions for all ROI’s, both for the position and the amplitude.

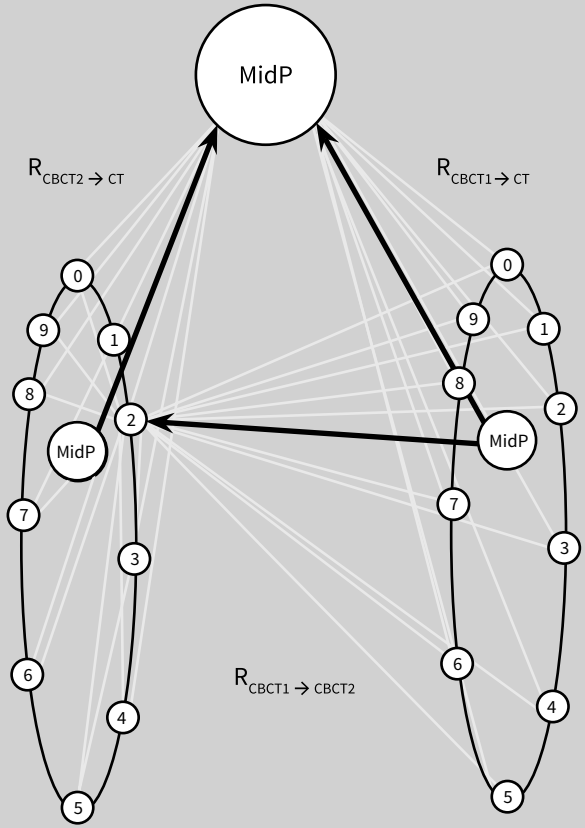
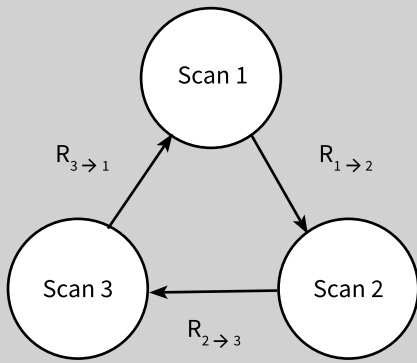


Figure A1a) Schematic representation of the full circle method for three 3D scans. b) adapted full circle method for the a 3D planning CT and two 4D CBCT scans.

Table A1: Results of the full circle method to quantify the registration accuracy for the time averaged mean position and the respiratory amplitude for the vertebrae, carina, marker, tumor.

	Position uncertainty			Amplitude uncertainty		
	LR (cm)	CC (cm)	AP (cm)	LR (cm)	CC (cm)	AP (cm)
Vertebrae	0.03	0.03	0.03	NA		
Carina	0.08	0.04	0.03	0.03	0.03	0.02
Marker	0.04	0.04	0.03	0.07	0.15	0.08
Tumor	0.07	0.08	0.03	0.03	0.03	0.04

APPENDIX REFERENCES

- A1. van Herk M, de Munck JC, Lebesque JV, et al.: Automatic registration of pelvic computed tomography data and magnetic resonance scans including a full circle method for quantitative accuracy evaluation. *Med Phys* 25:2054-2067, 1998